AIAA 81-1921R

Development of New Lifting-Parachute Designs with Increased Trim Angle

W.R. Bolton*
Sandia National Laboratories, Livermore, California
and
I.T. Holt† and C.W. Peterson‡
Sandia National Laboratories, Albuquerque, New Mexico

The trim angle of attack of a high-strength ribbon lifting parachute has been increased by a combination of modifications including increased liner area, increased slanted ribbon area, and the addition of flow-directing side vents. Ram air inflated leading-edge chambers were used to prevent canopy collapse at high angles of attack. Small-scale wind-tunnel models with the most beneficial combination of modifications had trim angles as high as $\alpha_t = 46$ deg. Full-scale parachutes had trim angles greater than $\alpha_t = 40$ deg in wind-tunnel and flight tests. Yaw-roll interaction was identified as a source of aerodynamic roll moment which would probably necessitate active control of roll orientation.

Nomenclature

C_d = drag coefficient = drag/(qS)
C_f = line force coefficient = force/(qS)
C_M = pitch moment coefficient = moment/(qSD)
CRM = roll moment coefficient = moment/(qSD)
CYM = yaw moment coefficient = moment/(qSD)
D = parachute constructed diameter
q = dynamic pressure = $\frac{1}{2}\rho V^2$
S = parachute reference area = $\pi D^2/4$
V = freestream velocity
α = parachute angle of attack
β = parachute sideslip angle
Δ = increment between body and parachute angular orientation
ρ = air density

Subscript

t = trim

Introduction

A LIFTING parachute is one with features causing it to trim at an angle of attack with respect to the direction of flight. As a result of this trim angle of attack, the total aerodynamic force of the parachute has a component normal to the direction of flight which may be used, if properly oriented, to lift the parachute and payload. In a typical application, the lifting parachute is deployed at high speed and low altitude, slowing and lifting the payload above the release altitude. At this point, sufficient altitude is available for deployment and inflation of a large second-stage parachute for descent to the ground. Because the second-stage parachute need not be deployed at high speed, it may be of light construction and designed for a low terminal velocity.

A parachute system as described above was developed as part of a weapon system in 1975-1978. Construction features of the lifting parachute developed during this program are shown in Fig. 1. The basic ribbon parachute was made to trim at a nonzero angle of attack by creating a porosity asymmetry. The ribbons on that side of the canopy in which lift was desired were lined with cloth, creating a local low-porosity region. Diametrically opposite the low-porosity region, a high-porosity region was created by inclining the ribbons relative to the basic canopy contour. The slanted ribbons act as a cascade, allowing increased flow through that portion of the parachute and deflecting the flow downward through a larger angle than would be possible without the slanted ribbons. The development of the basic ribbon lifting parachute is described in Ref. 1.

The basic ribbon lifting parachute eventually attained a trim angle of approximately $\alpha_t = 35$ deg, which seemed to represent the maximum achievable with that configuration. The activities described in this paper were an attempt to obtain increased lifting-parachute performance with an initial goal of $\alpha_t = 40$ deg. Such increase in trim angle would result in a significant increase in the ratio of parachute lift/drag. As will be discussed in a later section, other factors influence the performance of the system; however, this increase in lift/drag suggested a potentially useful improvement in system performance.

Efforts to increase parachute performance focused on increasing the asymmetric porosity distribution of the canopy and increasing the flow deflected while passing through the inflated parachute. Concepts considered to achieve these goals included increased liner area, vent pull-down, increased slanted ribbon area, increased slanted ribbon angle with respect to the canopy contour, and flow-directing side vents. From earlier development activities, it was recognized that as a lifting parachute is driven to higher angles of attack the differential pressure across the canopy liner diminishes, eventually leading to collapse of the parachute. Therefore, a second class of parachute modifications was considered to prevent collapse of the parachute at high angles of attack. These modifications included ram air inflated leading-edge chambers, flow-directing skirt extensions, circumferential shortening of the canopy across the liner, and radial shortening of the canopy across the liner. Certain of these concepts are illustrated in Fig. 2. The purpose of this paper is to give an overview of the evaluation process for these modifications which began with a series of small-scale wind-tunnel tests and led to flight testing of full-scale parachutes.

Small-Scale Wind-Tunnel Tests

Model parachutes approximately 1 m in constructed diameter embodying the concepts to be evaluated were

Submitted Oct. 14, 1981; presented as Paper 81-1921 at the AIAA 7th Aerodynamic Decelerator and Balloon Technology Conference, San Diego, Calif., Oct. 21-23, 1981; revision received Jan. 25, 1982.

*Member of Technical Staff, Tactical Systems Division.
†Member of Technical Staff, Retardation Systems Division. Member AIAA.
‡Supervisor, Retardation Systems Division. Member AIAA.

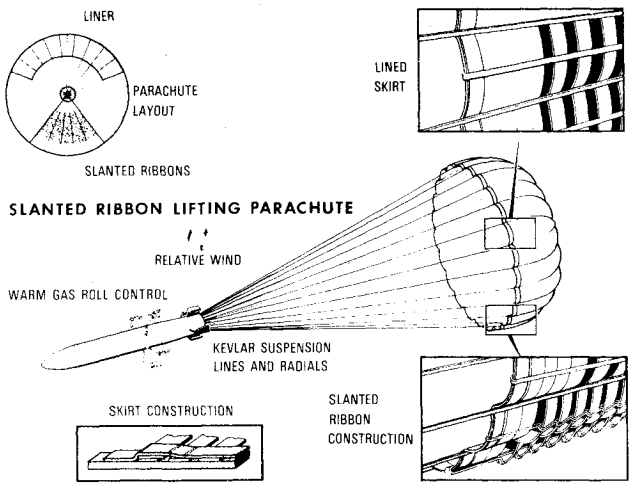

Fig. 1 Slanted ribbon lifting-parachute design features.

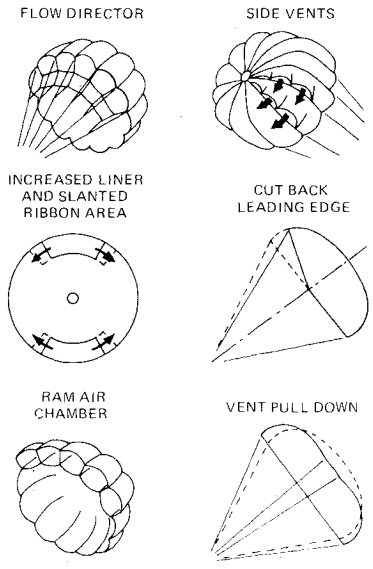

Fig. 2 Parachute modifications considered.

constructed of light flexible materials. These models were evaluated in a series of three wind-tunnel tests conducted at the Vought Corporation 7 × 10 ft low-speed wind tunnel. The small-scale wind-tunnel tests were conducted to identify promising configurations and measure their characteristics. Many concepts were discarded in the course of the tests as being unsuitable or requiring substantially more development than configurations offering comparable performance. The following brief comments summarize the observations from these wind-tunnel tests.

1) Ram air chamber. The ram air chamber reduced the tendency of the canopy leading edge to collapse at large trim angles, providing a margin of 3-5 deg between trim angle and the angle of attack for leading-edge collapse. On the 24 gore parachute, ram air chambers spanning 9 gores across the leading-edge liner were more satisfactory than 7 gore chambers.

2) Flow director. The flow director arranged somewhat like a skirt extension was positioned behind the lined leading edge of the parachute by auxiliary suspension lines attached to the main suspension lines. It was intended to act as a leading-edge dam, increasing the pressure differential across the skirt and preventing leading-edge collapse. However, the flow director forces, acting through the canopy suspension lines, tended to collapse the leading edge and reduce the parachute trim angle. Although it might prove effective if repositioned, other concepts appeared to be more satisfactory and the flow director was dropped from further consideration.

3) Side vents. The combination of increased side liner and flow-directing side vents significantly increased the trim angle of attack of the basic lifting parachute. The side vent configuration that provided the best combination of trim angle and stability was three vents along the side radials on each side of a 24 gore parachute.

4) Cutback leading edge. Removing a circular segment of the canopy leading edge up to 20% of the radial length in width reduced the tendency for leading-edge collapse. With the cutback leading edge, the margin between trim angle and the angle of attack for leading-edge collapse was 3-5 deg. However, this modification was accompanied by increased lateral oscillations of the parachute at trim.

5) Vent trim. By adjusting the vent pull-down line length, a 10% increase in the parachute trim angle was achieved. Based on steady-state trim angle and inflation line loads, the optimum vent pull-down line length was found to be approximately 1.2 times the suspension line length. At this line length, approximately 40% of the peak inflation load and 25% of the steady-state load are carried in the vent lines.

The most promising concepts from the small-scale wind-tunnel tests were embodied in four parachute designs selected for further evaluation. The four model parachutes were all of ribbon construction 1 m in diameter with 24 gores. The following features were added to each configuration.

Configuration A, differential porosity: liner from skirt to vent under seven leading-edge gores, 25% geometric porosity flat ribbons in five gores on each side of the canopy, and 50% geometric porosity flat ribbons in seven gores opposite the liner.

Configuration B, ram air chamber: ram air chamber on nine leading-edge gores, three side vents with 25% fullness in three gores on each side of the canopy, and slanted ribbons in five gores opposite the liner.

Configuration C, cutback leading edge: liner from skirt to vent under nine leading-edge gores, liner cutback in a circular arc across nine leading-edge gores (a maximum of 20% of radial length), side vents identical to configuration B, and slanted ribbons identical to configuration B.

Configuration D, slanted ribbon: liner 50% of radial length near skirt under seven leading-edge gores reduced to 25% of radial length under one additional gore at each end, 50% geometric porosity flat ribbons 25% of radial length near the skirt in five gores on each side of the canopy, and slanted ribbons 75% of radial length in five gores opposite the liner.

During the wind-tunnel tests, detailed measurements were made of canopy pressure distributions, suspension line forces, and parachute stability and damping characteristics. Model parachute inflations were conducted in the Vought low-speed wind-tunnel to investigate the inflation characteristics of the selected parachute designs. For inflation testing, the model parachutes were attached to a model body suspended by cables in the center of the wind-tunnel test section. The small-scale model parachute was reefed to a small diameter and allowed to stream behind the body as the wind tunnel was brought to the desired test condition. An electrically fired explosive squib cut the reefing line to initiate inflation. Simultaneous with disreefing, a flash bulb was fired to mark the start of inflation in high-speed motion pictures. Data were obtained from a body-mounted drag cell measuring total parachute drag force and from 12 line force gages measuring the line loads for pairs of suspension lines.

The inflations of the model parachutes typically exhibited an initial "overinflation," resulting in a peak drag force, followed by damped oscillations leading to the steady-state drag. The parachute structure must accommodate the peak inflation loads as well as the steady-state load. For this reason, the ratio of peak inflation load to steady-state load was of interest. Comparison of the drag histories for the low-porosity designs (configurations B and C) with those for the higher porosity basic ribbon lifting parachute showed a similar ratio of peak to steady-state drag force of 1.75/1.85.

A drag/time history representative of the low-porosity designs is shown in Fig. 3.

As previously mentioned, the tension in pairs of suspension lines was measured with line force gages. Line forces have been estimated in the past by measuring the total canopy drag force during inflation and assuming that the force is evenly distributed among the suspension lines. However, this approach overlooks the possibility that individual lines are more heavily loaded than the average based on total drag. Figure 3 shows the sum of the line forces for configuration B during inflation. Comparison of the two curves in Fig. 3 shows a good agreement between summed line forces and total drag. Note that wind axis drag coefficient measured by the drag cell is lower than the parachute axis axial force coefficient measured by the line force gages. These coefficients differ by the cosine of the parachute angle of attack allowed by the model support cables. Figure 4 summarizes the peak line forces measured around the canopy of configuration B during a typical inflation. In general, the peak line force is higher than that indicated by the total parachute drag averaged over all suspension lines. The estimate of line forces may be improved by correcting for the geometry of the suspension lines relative to the load cell sensitive axis. However, even this corrected load significantly underestimates the peak load in some lines.

A portion of the small-scale wind-tunnel tests were devoted to measuring the "off trim" restoring moments and forces. The resulting stability description of the parachute designs became an important part of the trajectory simulation used to predict system performance.[2] To measure its stability characteristics, each model was mounted on the six-component balance arrangement. The model parachute sting passed through the canopy vent and attached to a force and moment measuring balance. The balance and sting positioned the parachute at the desired attitude with respect to the relative wind in the tunnel test section. Reference 3 contains a more detailed description of the wind-tunnel instrumentation. Examination of the data gives an impression of the degree of stability of the parachute and its expected behavior when disturbed. Polynomial expressions were fitted to the stability data to provide aerodynamic models of the parachute designs for trajectory simulation. Selected stability characteristics for configuration B will be presented as being typical of the low-porosity lifting-parachute designs.

Pitching moment as a function of angle of attack is shown in Fig. 5. The condition for stable trim in pitch is the moment equal to zero and a positive slope of the pitch moment vs angle-of-attack curve. For configuration B, this condition is satisfied at approximately $\alpha = 47$ deg. The shape of the curve shown in Fig. 5 is typical for lifting parachutes with only the trim angle and maximum negative pitching moment changing for various designs.

Yaw characteristics are shown in Fig. 6. The conditions for a stable yaw trim are moment equal to zero and a positive slope of the yaw moment vs sideslip angle curve. It is typical for lifting parachutes to have an "N"-shaped yaw stability that is a function of angle of attack. That is, near zero angle of attack the parachute is unstable at zero sideslip and seeks stable trim points at large angles of sideslip. As the angle of attack approaches the trim angle, the stable yaw trim points move toward zero sideslip angle. The angle of attack for which the yaw becomes stable at zero sideslip angle is a function of parachute design: more asymmetric designs with large trim angles have a large angle of attack for yaw stability. The N-shaped yaw characteristic could result in lateral excursions when the parachute is at an angle of attack near zero, as during inflation prior to reaching trim angle of attack.

Figure 7 shows the roll moment of configuration B as a function of sideslip angle. Note that an increment in sideslip angle produces an increment in roll moment. Therefore, yaw excursions can produce roll moment as well as side force. Both of these effects are undesirable because they redirect the

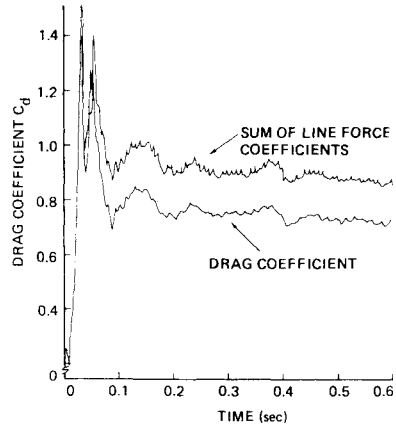

Fig. 3 Configuration B, inflation drag time history from small-scale wind-tunnel test.

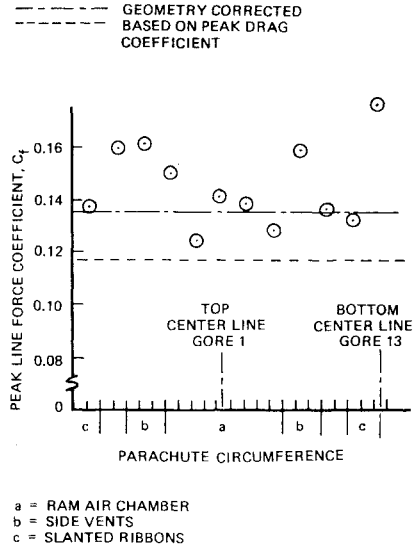

Fig. 4 Configuration B, peak inflation line forces.

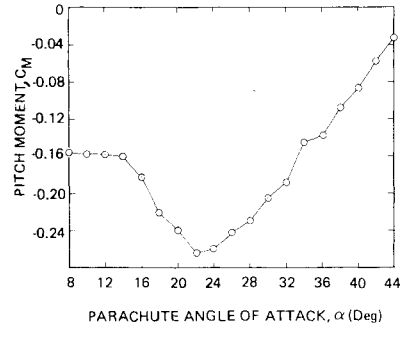

Fig. 5 Configuration B, pitch moment.

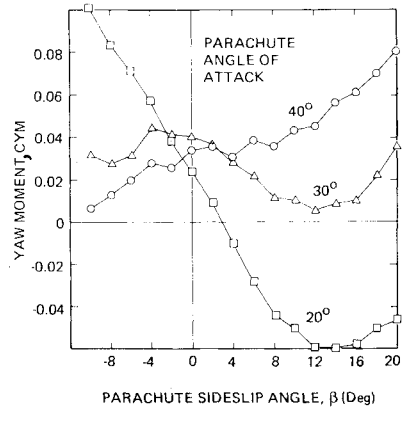

Fig. 6 Configuration B, yaw moment.

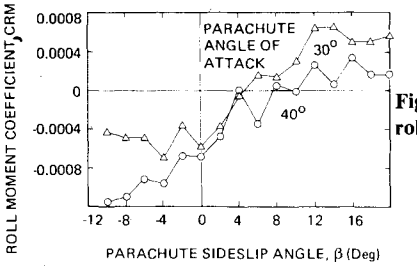

Fig. 7 Configuration B, roll moment.

parachute force in other than the desired direction. This yaw-roll interaction is unstable in that canopy sideslip angle will result in roll moment, tending to further increase the sideslip angle. Unfortunately, the more asymmetric low-porosity designs have undesirable lateral stability characteristics. Table 1 summarizes basic characteristics measured during small-scale wind-tunnel tests for the four parachute designs selected for further investigation.

Whirl Tower Tests

Whirl tower testing was undertaken as an intermediate step between wind-tunnel tests and full-scale flight tests. While not a substitute for flight testing, the whirl tower provides a full-scale flight test-like environment with a release velocity up to 170 m/s and a release altitude of 36 m above ground level. The whirl tower test method allows the selection of a realistic vehicle weight so that parachute inflations are not at "infinite mass" conditions as is typical of wind-tunnel inflations. One aspect of the whirl tower test environment can have a significant effect on parachute experiments. As the tower spins to the desired release velocity, the boom, cable, and test unit rotate together. At a release velocity of 170 m/s, the angular velocity of the test unit at release is 185 deg/s. Obviously, this high initial yaw rate can result in large yaw angles in the period between release and parachute inflation. With a test vehicle static margin of 10% of body length, the initial yaw excursion following release was limited to approximately 30 deg.

For whirl tower testing, 2.6 m diam parachutes of the four designs identified in small-scale wind-tunnel tests were constructed. The basic parachutes were of 20 deg conical shape and utilized continuous horizontal ribbon construction to get a maximum strength-to-weight relationship. Because of the higher basic porosity and better inflation, the differential porosity design required 9000 lb strength radials/suspension lines and 1500 lb horizontal ribbons. The other three, less porous, more asymmetric designs required 13,000 lb radials/suspension lines and 2000 lb horizontal ribbons. Kevlar was used in the radials, suspension lines, and skirt band. All other materials were nylon.

Test Observations

A total of 15 tests were conducted from the whirl tower on the four lifting-parachute configurations. The following observations were drawn from these tests.

Configuration A, differential porosity: This parachute design exhibited consistent and orderly deployment and inflation, and had relatively low roll rates during the whirl tower tests, indicating low parachute rolling moment. However, this design had a trim angle approximately the same as earlier lifting parachute designs.

Configuration B, ram air chamber: The ram air chamber parachute inflated well and had the highest trim angle of any parachute tested at the whirl tower. There was no indication of ram air chamber collapse or asymmetric inflation but the parachute did have large roll rates.

Configuration C, cutback leading edge: During the whirl tower test, the cutback leading-edge parachute showed poor inflation characteristics and large lateral and pitch oscillations, and failed to achieve a stable trim angle. The leading-edge cutback was significantly more severe, at 27% of radial length, than the 20% cutback intended for the small-scale models. Small-scale wind-tunnel data indicate a reduced pitching moment near zero angle of attack. With a more severe leading edge cutback, the parachute may fail to reach a trim angle because of the reduced pitch moment.

Configuration D, slanted ribbon: This design exhibited periodic leading-edge collapse, resulting in successive cycles of parachute collapse and reinflation in all of the configurations tested during the whirl tower tests. This behavior was in marked contrast to the well-behaved small-scale wind-tunnel model. Several configurations of vent lines were tested in this parachute design, but any effect of this modification was masked by the canopy oscillations.

Following the whirl tower tests, the parachutes were carefully inspected. Although minor deviations from the design intent were found, none appeared to be sufficient to explain the poor performance of configurations C and D. Because of the more encouraging performance of other designs, these designs were given reduced emphasis. However, based on the results of wind-tunnel tests, it appears that the vent pull-down concept has merit when applied to a stable lifting parachute. With further development, vent pull-down could offer significantly improved performance for a proved lifting-parachute design. The differential porosity design was quite satisfactory, although it did not offer improved trim angle over earlier designs. The ram air chamber appeared to provide high trim angle and good inflation characteristics but, based on wind-tunnel tests, might have undesirable stability characteristics. From the whirl tower test series, the ram air chamber design was selected as having the greatest potential for further development.

System Optimization

The performance of a lifting-parachute delivery system is intimately tied to the ratio of system lift/drag or L/D. System L/D is affected by body characteristics. Efforts to improve L/D, and hence system performance, naturally center on improving parachute lift, but the importance of the body contribution should be recognized. In the usual and most convenient arrangement, the lifting parachute is attached to the aft end of the body. When the parachute reaches its trim angle of attack, the body is held at a large negative angle of attack. As a result, body drag increases system drag and body lift decreases system lift, reducing the system L/D from that characteristic of the parachute alone.

Parachute and body aerodynamic characteristics have been measured during wind-tunnel tests. The body shape assumed in the following discussion is that of the lifting-parachute flight test vehicle. Figure 8 shows wind-tunnel test results for several lifting-parachute designs of different configurations. Although these parachutes have a range of lift/drag ratios, their characteristics follow a remarkably similar curve of L/D vs angle of attack. This curve is the justification for the assumption that parachute L/D is uniquely linked to canopy angle of attack and that lifting parachutes may be constructed with any desired trim angle up to approximately 45 deg. The data points and solid curves represent the lifting performance of parachute models measured in small-scale wind-tunnel tests. The locus of trim angles of attack, and the corresponding L/D as measured for unrestrained parachutes in the wind tunnel, is shown by the broken line. Comparison of the solid and broken lines suggests that the peak L/D for a parachute occurs at a somewhat lower angle of attack than trim. The dashed line represents the tangent of the parachute angle of attack. If it is assumed that the resultant force vector is aligned with the parachute axis of symmetry, then $\tan(\alpha)$ represents the parachute L/D. Comparison of the broken and dashed lines in Fig. 8 shows that at trim the resultant force is, in fact, not aligned with the parachute axis of symmetry and this assumption results in an overestimate of the parachute L/D.

Table 1 Small-scale wind-tunnel model parachute characteristics

Configuration	Description	Trim angle, α_t, deg	Inflation load ratio, peak/steady state
A	Differential porosity	29	1.6
B	Ram air chamber	46	1.8
C	Cutback leading edge	46	1.7
D	Basic ribbon lifting	32	1.8
D	Vent pull-down	37	1.6

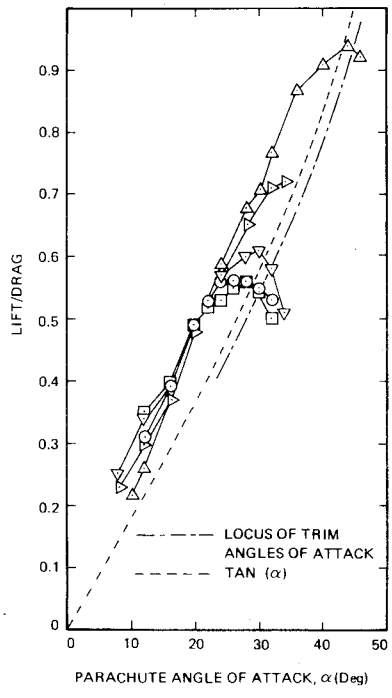

Fig. 8 Lifting-parachute lift/drag based on small-scale wind-tunnel data.

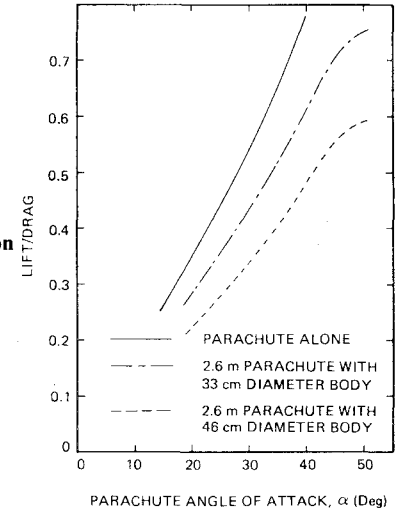

Fig. 9 Effect of body on system lift/drag.

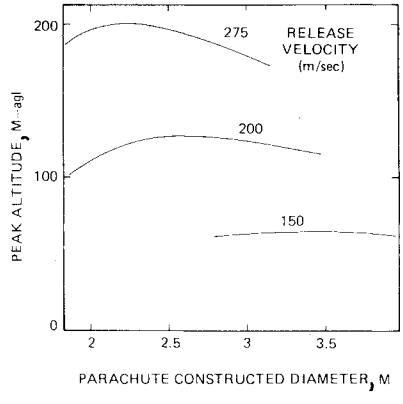

Fig. 10 System performance for parachute lift/drag = 0.65.

Body and parachute wind-tunnel data may be used to show the effect of the body on system L/D. Figure 9 shows a comparison of system L/D and parachute L/D as a function of parachute angle of attack. The solid line represents the L/D of the parachute undegraded by the presence of the body. This curve represents the highest value that the system L/D could obtain if the body had neither lift nor drag. The interval between the solid line and the broken and dashed lines is the reduction in system L/D attributable to the body. Comparison of the broken line (representing a 0.46 m diam body) and the dashed line (representing a 0.33 m diam body) shows that the effect of the body is reduced as it becomes smaller in relation to the parachute. For a fixed parachute trim angle, system L/D may be increased by a design tending to minimize body lift and drag—one, for example, having a minimum body size and a forward center of gravity minimizing fin size for the required level of body stability.

With a given level of parachute performance and the body design specified, there remains the matter of sizing the parachute to obtain the best system performance. While there are several possibilities, the measure of system performance adopted is the peak altitude reached during the lifting parachute trajectory. The sensitivity of this performance measure to parachute size was investigated using a computer trajectory simulation.[2] A typical relation between peak altitude, release velocity, and parachute size based on trajectory simulations is shown in Fig. 10. This figure shows that for a fixed release velocity there is a fairly strong interaction between parachute size, minimum peak altitude required, and system weight. Reduced delivery velocity, increased system weight, and reduced system L/D all result in increased optimum parachute size. As is clear in Fig. 10, a given parachute size will be optimum at only one release velocity. It is generally advantageous to select the optimum parachute for the minimum required release velocity. At higher velocities, the parachute will give suboptimal performance, but the increased kinetic energy will still result in increased peak altitude.

Full-Scale Wind-Tunnel Tests

To obtain comparative data on canopy lift, rolling moment, yaw damping, and inflation characteristics in a controlled environment with instrumentation that could not be used in subscale wind-tunnel or whirl tower tests, 2.6 m lifting parachutes were tested in the NASA Ames 40×80 ft wind tunnel. A full-scale model of the payload (an ogive cylinder with T-fins) was mounted on the standard 40×80 ft wind-tunnel struts for this test. The model was 46 cm (18 in.) in diameter and 3.66 m (12 ft) long. Potentiometers measured the model pitch and yaw angles. Parachute axial force and roll moment were measured by strain gages located within the forebody. Reference 3 provides more details on the forebody and test setup. Measurements of parachute pitch, yaw, and roll relative to the forebody were accomplished using a small computer-controlled video camera mounted on the model base. Reference 4 provides more information on the computerized video data system and presents typical parachute performance data plots.

In addition to measurements of parachute performance at trim conditions, the dynamic behavior of the full-scale lifting parachutes was studied during inflation and during the return to the trim position from a large initial yaw angle. High-speed film coverage, parachute loads, and forebody motion data were obtained at a dynamic pressure of 1.68 kPa (35 psf) for both inflation and yaw damping tests.

Table 2 summarizes the performance of all full-scale lifting-parachute configurations at their trim conditions. The measured trim angles of attack are for the full-scale canopy configurations. The exception to this statement is the cutback leading edge canopy (configuration C), which did not inflate to trim angle of attack.

Other observations on the performance of the full-scale lifting parachutes in the 40×80 ft wind tunnel are summarized below.

Configuration A, differential porosity: Full-scale wind-tunnel data confirmed the whirl tower and subscale wind-tunnel results. The differential porosity lifting parachute exhibited well-behaved dynamic characteristics, but it had insufficient lift to warrant further considerations for the present application.

Configuration B, ram air chamber: The ram air chamber canopy achieved the highest trim angle of any configuration, as it did in all previous tests. The canopy has lower effective porosity than the other configurations, as evidenced by its higher axial force coefficient. Its inflations were symmetric and the canopy roll coefficient was the lowest of all configurations tested. The canopy showed some "breathing" at its trim angle of attack of 42 deg. When released from an off-trim yaw angle of 15 deg, the canopy oscillated in yaw with no apparent damping. The parachute must generate lateral forces which make it appear to have zero yaw damping.

Configuration C, cutback leading edge: The cutback leading-edge canopy could not assume its trim angle of attack in the wind tunnel. The parachute canopy was inflated and flew at a large negative angle of attack as the tunnel airspeed was increased. The removal of part of the leading edge of the liner at the top of the parachute prevented the canopy from generating enough lift to reach a positive trim angle of attack.

Configuration D, slanted ribbon: The slanted ribbon canopy was tested with and without vent pull-down lines. Without vent pull-down lines, the parachute trimmed at 36 deg with very little canopy roll torque. Off-trim initial yaw angles were damped out in one cycle. The use of successively shorter vent pull-down lines increased the trim angle to over 41 deg and the axial force coefficient from 0.60 to 0.69. The canopy showed little motion or leading-edge collapse at trim conditions with the vent pull-down lines present, in contrast to whirl tower test results. High stress concentrations were observed where the pull-down lines were attached near the canopy vent band. Unfortunately, the slanted ribbon canopy with a 2.79 m (110 in.) pull-down line was completely unstable during inflation. As the parachute opened, it generated lifting forces which caused the canopy to fly above its maximum pitch angle of attack. Once it exceeded this maximum pitch angle, the canopy collapsed and lost all lift. As the canopy reinflated, the process was repeated. The rapid pitch-up, collapse, and rebound motion was uncontrollable and caused damage to the wind-tunnel model.

On the strength of its excellent performance in subscale wind-tunnel, whirl tower, and the 40×80 ft wind-tunnel tests, the ram air chamber canopy configuration was selected for the flight test program. The differential porosity canopy demonstrated excellent flying characteristics and should be considered for applications requiring a relatively inexpensive lifting parachute with $L/D \leq 0.62$. Further refinements of the cutback leading-edge canopy and slanted ribbon canopy with vent pull-down lines are necessary before those configurations should be considered for use in a weapons system.

Flight Tests

Three flight tests have been conducted on a high-lift parachute design. The parachute selected for flight test was the ram air chamber design configuration B. This parachute appeared to offer the best combination of trim angle and stability during the whirl tower evaluations. To minimize test costs, the same parachutes tested at the whirl tower and for the full-scale wind-tunnel tests were reused for flight tests. The only modification to the parachute was replacement of the suspension lines with longer lines suitable for the flight test vehicle.

The test vehicle consisted of modified components from an earlier lifting-parachute test series. Using existing components reduced the cost of flight tests but resulted in a combination of vehicle aerodynamics, weight, and parachute size that was not optimum. The test vehicle contained an instrumentation system which measured body angular orientation, angular rates, and linear accelerations and monitored the functioning of an on-board roll control system used to maintain the proper orientation of the parachute lift vector. These measurements were transmitted to a ground station where they were recorded for subsequent analysis.

Flight tests were conducted from a Navy A-7 aircraft at the Department of Energy test range at Tonopah, Nev. Table 3

Table 2 Full-scale lifting parachute performance in the NASA Ames 40×80 ft tunnel

Canopy configuration	Config.	α_t, deg	$\Delta\alpha_t$, deg	β_t, deg	$\Delta\phi$, deg	$CRM \times 10^4$	C_A
Differential porosity canopy	A	32.0	2.9	−0.7	−3.2	−0.42	0.56
Ram air chamber canopy	B	42.2	3.8	−0.1	−0.8	−0.13	0.78
Cutback leading-edge canopy	C	Would not reach trim conditions in the tunnel starting at a negative canopy angle of attack					
Slanted ribbons, no vent line	D-0	36.2	2.1	−1.5	+4.5	−0.23	0.56
Slanted ribbons, 3.05 m vent line	D-1	38.2	4.3	−1.8	−1.2	−0.18	0.60
Slanted ribbons, 2.79 m vent line	D-2	40.6	4.0	+0.5	−1.5	−0.21	0.69
Slanted ribbons, 2.54 m vent line	D-3	41.1	3.6	−1.6	−1.6	−0.47	0.68

Table 3 Lifting parachute flight test conditions

	FTU-1	FTU-2	FTU-3
Altitude			
Above ground level, m	464	471	444
Mean sea level, m	2095	2099	2072
Velocity			
Calibrated airspeed, knot	483	481	475
True airspeed, knot	527	525	518

summarizes the release conditions for these tests.

The results of these flight tests are briefly described below.

FTU-1

Although the FTU-1 parachute had survived whirl tower deployment at 334 knots, the higher dynamic pressure of the aircraft release resulted in partial failure of the ram air chambers at inflation. As the canopy became fully inflated, the ram air chambers failed at their vent end and separated from the canopy toward the skirt.

In preparation for FTU-2, the remaining ram air chamber parachute was reinforced to prevent the failure observed in FTU-1. These modifications were intended to provide adequate structural paths for loads imposed on the ram air chamber to be transmitted to the radials and ribbons of the canopy. In addition, design and procurement were initiated for a new parachute of the same ram air chamber design with high-lift features better integrated with basic parachute structure for use in a third flight test.

FTU-2

The modified ram air chamber parachute survived the FTU-2 flight test with no evidence of structural distress. The parachute trim angle, as measured from documentary motion pictures, was approximately 42 deg. The parachute inflated well and maintained a good inflated shape. However, in the last second of the lifting phase, the canopy experienced positive sideslip angle and roll moment in excess of the roll control system torque, resulting in a roll excursion of approximately 90 deg.

FTU-3

The improved structural design withstood the loads of flight test with no damage. Deployment and inflation of the parachute were normal; but after reaching trim angle of attack of approximately $\alpha_t = 41$ deg, negative rolling moment resulted in roll through 720 deg. In all flight tests, the second-stage parachute performed as desired and the test unit was recovered undamaged.

Conclusion

Several concepts have been identified that can give significant increase in trim angle, notably: increased liner area, side vents, increased slanted ribbon area, ram air chambers, and vent pull-down. Although not all of the concepts identified were developed in this program, the combination of features embodied in the ram air chamber parachute demonstrated a trim angle of over 45 deg in small-scale tests and over 40 deg in full-scale flight tests. This performance represents approximately 25% increase in parachute lift/drag over earlier lifting parachute designs.

During flight test, parachute roll moments were observed that were larger in magnitude than the torque available from the roll orientation system. On the basis of wind-tunnel data, the source of this roll moment appears to be a yaw-roll interaction which is made more severe by the same parachute modifications that produced large trim angles. Previous experience with lower trim angle parachutes shows that the undesirable roll behavior may be controlled by a sufficiently powerful roll control system. For a particular application, the optimum design will involve a compromise between trim angle for the desired lift and acceptable lateral characteristics to minimize the required roll control torque.

Acknowledgments

The authors wish to express appreciation for the assistance of M.T. Ferrario, L.D. Whinery, H.E. Widdows, and members of the Experimental Aerodynamics and Flight Test Instrumentation Divisions of Sandia National Laboratories in preparation for and conduct of lifting parachute test activities. This work was supported by the U.S. Department of Energy.

References

[1] Rychnovsky, R.E., "A Lifting Parachute for Very Low Altitude, Very High Speed Deliveries," AIAA Paper 75-1389, Nov. 1975.

[2] Bolton, W.R., "Trajectory Simulation for a Lifting Parachute System," AIAA Paper 79-0470, March 1979.

[3] Croll, R.H., Klimas, P.C., Tate, R.E., and Wolf, D.F., "Summary of Parachute Wind Tunnel Testing Methods at Sandia National Laboratories," AIAA Paper 81-1931, Oct. 1981.

[4] Croll, R.H., Berg, D.E., and Johnson, C.S., "Computerized Video Instrumentation Technique for Wind Tunnel Testing of Parachutes," AIAA Paper 81-1929, Oct. 1981.